circuit representation of MSSW excitation can be obtained without resorting to the computational complexity of a full Maxwell equation—boundary value problem approach. Although the radiation resistance is a complicated function, it is of analytic form and thus is readily evaluated for a wide range of experimental conditions. The radiation reactance can be obtained from a numerical Hilbert transform of the resistance with little extra computational effort. Finally, the third element of the model can be derived from the characteristic impedance and guide wavelength of the microstrip line in the absence of MSSW excitation.

It is, unfortunately, not possible to draw a set of universal curves showing the dependence of Z_m on the various geometrical and material parameters. In this paper we have shown only those curves relevant to our experimental parameters to demonstrate the validity of the model; in general, Z_m must be calculated for each set of parameters of interest. However, from (4), (5), (6), and (9) it can be seen that, for a given bias field, $Z_m(\omega)$ does not change if the microstrip width b, dielectric thickness t, and magnetic layer thickness d are simultaneously scaled by a constant factor.

The experiments show that the equivalent circuit model is most effective for relatively wide stripwidths, but it accurately predicts the peak radiation resistance in all cases examined. For narrow strips, the correct qualitative dependence upon geometrical parameters is observed, but the bandwidth of the radiation resistance is consistently overestimated. The radiation reactance therefore also differs significantly from the predicted response. Despite these limitations, we believe the model to be a useful guide in the design of MSSW devices, both in selecting optimum geometrical parameters for the desired application and in designing appropriate matching circuitry.

ACKNOWLEDGMENT

The authors are indebted to A. Braginski of the Westinghouse Research Laboratories and H. Glass of the Electronics Research Division of Rockwell International for providing the YIG samples.

REFERENCES

[1] A. K. Ganguly and D. C. Webb, "Microstrip excitation of magnetostatic surface waves: Theory and experiment," *IEEE Trans. Microwave Theory Tech.*, vol. MTT-23, pp. 998–1006, Dec. 1975.
[2] A. L. Nalamwar and M. Epstein, "Immittance characterization of acoustic surface-wave transducers," *Proc. IEEE*, vol. 60, pp. 336–337, Mar. 1972.
[3] E. A. Guillemin, *The Mathematics of Circuit Analysis*. New York: Wiley, 1949, pp. 330–349.
[4] R. F. Mitchell and N. H. C. Reilly, "Equivalence of δ-function and equivalent circuit models for interdigital acoustic-surface-wave transducers," *Electron. Lett.*, vol. 8, no. 13, pp. 329–330, June 1972.

Harmonic Analysis of SAW Transducers

CARL M. PANASIK AND BILL J. HUNSINGER

***Abstract*—The excitation function of an unapodized interdigital transducer (IDT) is determined by measuring the discrete impulse response, taking into account the first seven harmonics of the frequency domain. Using a time-segregation method, all non-SAW time-domain components are suppressed. A single transducer is isolated by a method of autodeconvolution that utilizes a theoretically derived phase function. The resulting excitation function provides experimental insight into the operation of IDT electrodes and compares well with the theoretical response of Smith and Pedler [3]. The basic analysis technique can be used for other configurations, once the frequency-domain phase response of one transducer is known.**

I. INTRODUCTION

AN EXPERIMENTAL analysis technique has been devised which produces the time-domain excitation function of an isolated interdigital transducer (IDT). The time-domain excitation function is defined as the instantaneous surface acoustic wave (SAW) amplitude displacement distribution resulting from a voltage impulse applied to the transducer. Works of Engan [1], Hartmann and Secrest [2], Smith and Pedler [3], Bahr and Lee [4], and Szabo *et al.* [5] have presented theoretical descriptions of the SAW electric fields produced by the IDT.

This paper describes a technique for measuring the SAW amplitudes produced by these driving source fields. The time-domain excitation function is found by measuring the transducer frequency-domain voltage transfer ratio in a low impedance system and transforming it to produce the time-domain SAW amplitude distribution resulting from the driving source fields.

Manuscript received July 12, 1977; revised February 2, 1978. This work was supported by the Air Force Avionics Laboratory under Contract F33615-75-R-1291 and by JSEP under Contract DAASB-07-72-C-0259.

The authors are with the College of Engineering, University of Illinois at Urbana–Champaign, Urbana, IL 61801.

II. SAMPLED TIME-DOMAIN CALCULATIONS

The frequency-domain transfer ratio is measured for the distinct purpose of being transformed to the time domain. The frequencies at which the transfer functions

0018-9480/78/0600-0447$00.75

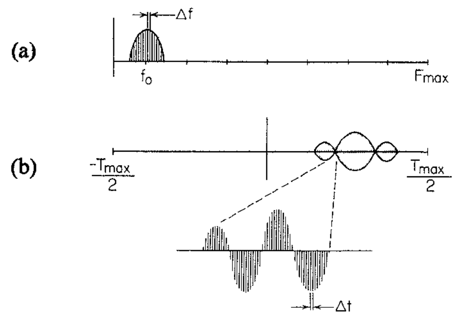

Fig. 1. (a) Frequency-domain sampling. (b) Time-domain sampling and increased time resolution.

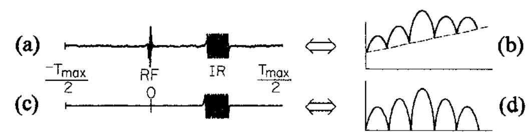

Fig. 2. Segregation of time-limited responses. (a) Original time domain. (b) Original frequency domain. (c) SAW time components. (d) SAW frequency response.

are measured must be sufficiently close together to account for the longest time delay component in the impulse response. The sampling theorem assures that no errors arise in the transform if the frequency measurements are taken at a spacing of

$$\Delta f \leqslant \frac{1}{T_{\max}} \tag{1}$$

where $T_{\max}$ is the maximum time range of the impulse response (Fig. 1). The digital Fourier transform is circular and

$$h(t)_{\text{calc}} = \sum_{i=1}^{\infty} h(t + T_{\max} \cdot i)_{\text{act}} \tag{2}$$

where $-T_{\max}/2 \leqslant t \leqslant T_{\max}/2$ produces an overlay of all time where $h(t)_{\text{calc}}$ is the calculated impulse response and $h(t)_{\text{act}}$ is the actual impulse response. If $T_{\max}$ is chosen greater than the longest actual time delay component, $h(t)_{\text{calc}}$ uniquely describes the entire impulse response without time-domain aliasing.

The maximum frequency measured ($F_{\max}$) establishes the separation between the samples (Δt).

$$\Delta t = 1/F_{\max}. \tag{3}$$

The total number of required measurement points is

$$N = \frac{T_{\max}}{\Delta t} = \frac{F_{\max}}{\Delta f} = T_{\max} \cdot F_{\max}. \tag{4}$$

III. Segregation of Time-Limited Responses

SAW delay line impulse responses like that shown in Fig. 2(a) are made up of multiple time-limited signals that occupy individual nonoverlaying time regions. The direct RF coupling [$h_{\text{RF}}(t)$] and the delay line impulse response [$h_{\text{IR}}(t)$] make up the complete transform of the measured transfer function $H(\omega)$ shown in Fig. 2(b):

$$H(\omega) = \mathcal{F}\left[h_{\text{RF}}(t) + h_{\text{IR}}(t)\right]. \tag{5}$$

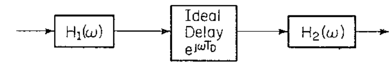

Fig. 3. Transfer function representation of a SAW device.

The complete delay line impulse response is calculated by taking the inverse transform of the measured frequency response. The SAW impulse response is segregated by suppressing all time regions of the impulse response except for the transducer direct impulse response (Fig. 2(c)). Transforming back to the frequency domain produces the isolated SAW mode transfer function shown in Fig. 2(d). The number (N') of points used in this calculation is reduced to

$$N' = F_{\max} \cdot T'_{\max} \tag{6}$$

where $F_{\max}$ defines the original frequency range and $T'_{\max}$ is the time duration of the nonsuppressed impulse response.

Surface acoustic wave devices consist of two transducers operating in cascade (Fig. 3). If the propagation is nondispersive and diffraction free, the transfer functions of individual transducers multiplied together produce the delay line transfer function

$$H(\omega) = H_1(\omega) \cdot H_2(\omega) \cdot \exp(j\omega T_D) \tag{7}$$

where $H_1(\omega)$ is the transfer function of the input transducer, $H_2(\omega)$ is the transfer function of the output transducer, and T_D is the time delay. The delay is removed by taking the phase slope out of the measured frequency data.

The response of transducer 2 may be written as

$$H_2(\omega) = \frac{H(\omega)}{H_1(\omega)}. \tag{8}$$

To solve (8), $H_1(\omega)$ must be known. In general, neither $H_1(\omega)$ nor $H_2(\omega)$ is experimentally known, but for the case where the transducers are identical and unapodized, (8) reduces to the autodeconvolution

$$H_2(\omega) = \sqrt{H(\omega)}\ . \tag{9}$$

In the process of autoconvolution, the frequency phase function is doubled, and phase values of π become $2\pi = 0$ and, therefore, cannot be recovered by the inverse process of autodeconvolution. Additional phase information must be added for the autodeconvolution to produce a unique single transducer response.

IV. Experimental Results

The device selected for harmonic analysis has two 15-wavelength apertures, six double-electrode transducers separated by approximately 100 wavelengths. These aluminum fingers are deposited on a 20-mil thick $LiNbO_3$ substrate and have a stripe-to-space ratio of 0.388. The back surface has been grooved at 45° to scatter deep bulk waves.

The time-domain analysis system [6] enables one to accurately measure the effective tap weights and delays of a SAW filter in a form compatible to computer analysis. Along with the first-order response, the tap weight and

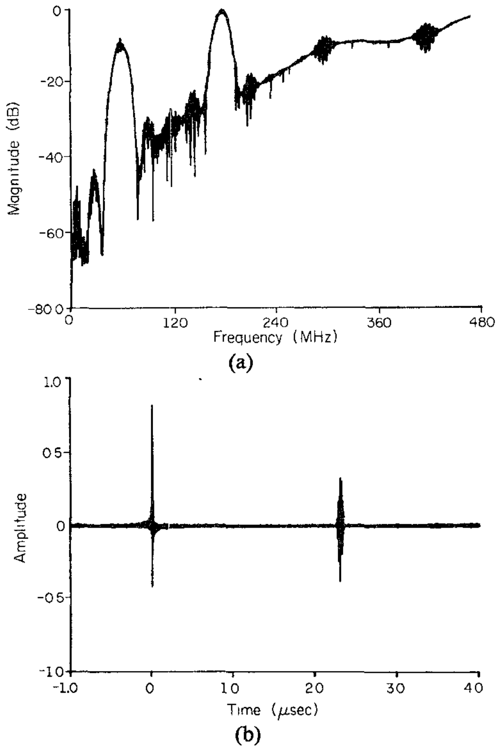

Fig. 4. Original measured harmonic data. (a) Frequency domain with RF coupling. (b) Impulse response.

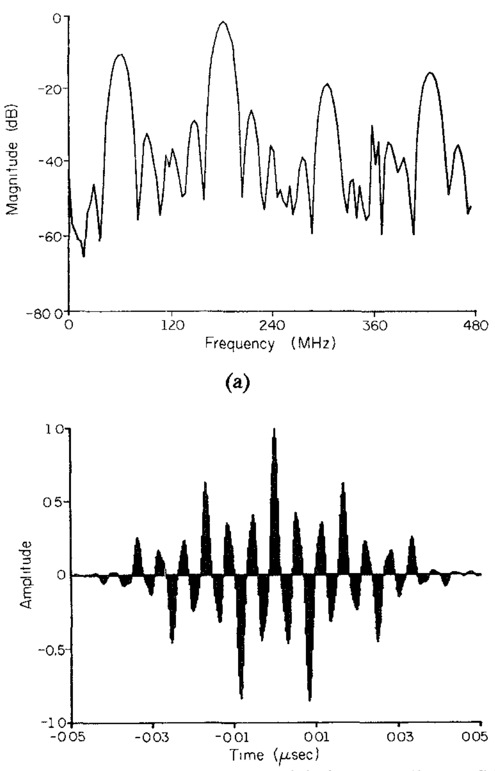

Fig. 5. (a) Frequency response after deletion of all non-SAW time components. (b) Expanded impulse response at $t=0$.

(b)

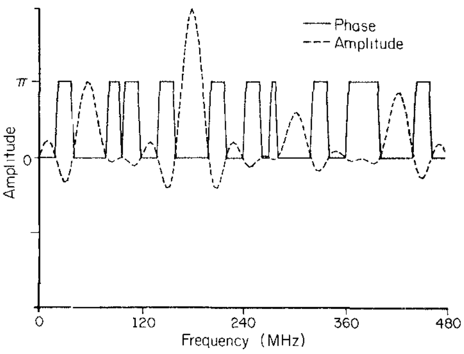

Fig. 6. Theoretically derived phase function.

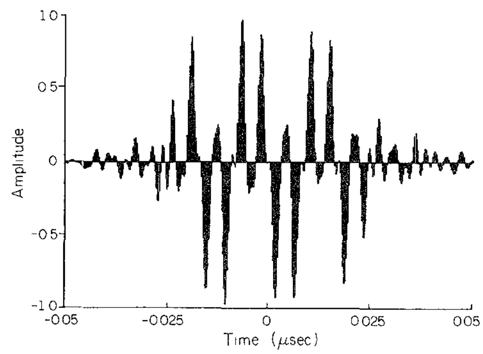

Fig. 7. Experimentally calculated excitation function.

delay data take into account all higher order transducer responses such as regenerations, reflections, diffraction, and bulk modes. The original frequency-domain data (Fig. 4(a)) have a considerable RF coupling contribution (Fig. 4(b)). The SAW mode is isolated by the suppression of all non-SAW time components (Fig. 5(a)), while time delays are removed by adjustments to the phase slope (Fig. 5(b)).

Assuming that the processes of generation and detection are identical, separation of the two identical unapodized transducer responses is performed by autodeconvolution (9). The previously mentioned phase ambiguity is removed by the introduction of a π phase shift where anticipated from the phase of a calculated single transducer harmonic response. This response is not the transform of a theoretical impulse response. In that case, the magnitudes of each harmonic would be equal, giving an inaccurate representation. Rather, the frequency response used for phase crossover determination is created by the addition of four sinc(ω) functions centered at each harmonic and magnitude weighted by the experimental magnitude $[H_2(\omega)]$ at that harmonic (Fig. 6). The phase of this composite response is subtracted from the phase of $H(\omega)$, leaving the phase function of a single transducer. Relative phase offsets between harmonics are adjusted to the theoretical values determined by Hartmann and Secrest [2, Fig. 2]. Further work to resolve these phase ambiguities is required for the general case where the transducers are not identical and the relative weights of each transducer's harmonic response is not individually known. Before Fourier transforming, the time resolution is expanded by appending zeroes to the frequency-domain data. The result is the measured excitation function for a six double-electrode unapodized IDT (Fig. 7).

The impulse response of two double electrodes at the center of the transducer (Figs. 8(a) and (b)) is compared with the theoretical time response predicted by Hartmann and Secrest (Fig. 8(b)), and the time response predicted by

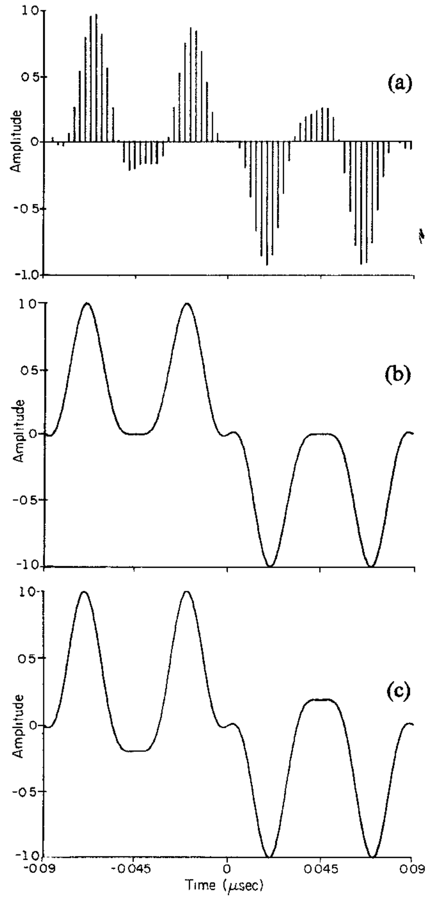

Fig. 8. Comparison with four-term Fourier series expansion. (a) Excitation function of two double electrodes. (b) Hartmann and Secrest. (c) Smith and Pedler.

Smith and Pedler (Fig. 8(c)). Both theoretical responses are calculated from the first four terms of the Fourier series expansion and are for a stripe-to-space ratio of 0.388. The predicted response of Smith and Pedler [3] more closely compares with this experimental data than that of Hartmann and Secrest [2].

V. Conclusion

The excitation function of an unapodized interdigital transducer is determined by measuring the discrete impulse response, taking into account the first seven harmonics of the frequency domain. Using a time-segregation method, all non-SAW time components are suppressed. A single transducer is isolated by a method of autodeconvolution which utilizes a theoretically derived phase function. The resulting excitation function provides experimental insight into the operation of IDT electrodes. For the case of two identical six double-electrode IDT's, the comparison with the theory of Smith and Pedler [3] is striking. The basic analysis technique can be expanded to nonidentical transducers and other electrode configurations, once the phase response of one transducer is known.

References

[1] H. Engan, "Excitation of elastic surface waves by spatial harmonics of interdigital transducers," *IEEE Trans. Electron Devices*, vol. ED-16, pp. 1014–1017, Dec. 1969.

[2] C. S. Hartmann and B. G. Secrest, "End effects in interdigital surface wave transducers," in *Proc. 1972 IEEE Ultrasonics Symp.*, pp. 413–416, Oct. 4–7, 1972.

[3] W. R. Smith and W. F. Pedler, "Fundamental- and harmonic-frequency circuit-model analysis of interdigital transducers with arbitrary metallization ratios and polarity sequences," *IEEE Trans. Microwave Theory Tech.*, vol. MTT-23, Nov. 1975.

[4] A. J. Bahr and R. E. Lee, "Equivalent circuit model for interdigital transducers with varying electrode widths," *Electron. Lett.*, vol. 9, pp. 281–282, June 28, 1973.

[5] T. L. Szabo, K. R. Laker, and E. Cohen, "Accurate IDT design using spectral weighting," in *Proc. 1976 IEEE Ultrasonics Symp.*, pp. 543–546, Sept. 1–Oct. 1, 1976.

[6] C. M. Panasik and B. J. Hunsinger, "Precise impulse response measurement of SAW filters," *IEEE Trans. Sonics Ultrason.*, vol. SU-23, July 1976.